



*Supplement of*

**A regional physical–biogeochemical ocean model  
for marine resource applications in the Northeast  
Pacific (MOM6-COBALT-NEP10k v1.0)**

**Elizabeth J. Drenkard et al.**

*Correspondence to:* Elizabeth J. Drenkard ([liz.drenkard@noaa.gov](mailto:liz.drenkard@noaa.gov))

The copyright of individual parts of the supplement might differ from the article licence.

**Table S1. Kling-Gupta Efficiency and Components for Timeseries Figures.**

The Kling-Gupta Efficiency (KGE) is calculated as:

$$KGE = 1 - \sqrt{(r - 1)^2 + (\alpha - 1)^2 + (\beta - 1)^2}$$

Where  $r$  is the Pearson correlation coefficient,  $\beta$  is the relative bias, and  $\alpha$  is the relative variance.

		KGE	r	$\beta$	$\alpha$
Figure 17: Surface and Bottom Temperature Comparisons (NEP10k vs. GLORYS) for the Shelves (depths between 0-500m) of the Regions Outlined in Figure 1					
BS	Surface	0.888	0.998	0.932	1.089
	Bottom	0.923	0.994	1.014	1.075
GOA	Surface	0.900	0.997	0.929	1.070
	Bottom	0.830	0.961	0.983	1.164
BC	Surface	0.841	0.993	0.981	1.157
	Bottom	0.780	0.889	0.967	0.813
NCCS	Surface	0.869	0.978	0.993	1.129
	Bottom	0.906	0.913	0.963	0.995
CCCS	Surface	0.874	0.886	1.053	1.010
	Bottom	0.847	0.857	0.950	1.020
SCCS	Surface	0.876	0.940	1.027	1.105
	Bottom	0.724	0.775	0.936	0.854
Figure 18: Regional Chlorophyll Timeseries Comparisons (NEP10k vs. ESA OC-CCI) for the Geographic Regions Outlined in Figure 1					
BS		0.609	0.792	1.208	1.258
GOA		0.564	0.900	1.336	1.259
BC		0.698	0.860	1.005	1.267
NCCS		0.745	0.805	0.913	1.141
CCCS		0.660	0.673	0.920	1.047
SCCS		0.526	0.640	0.940	0.698
Figure 20: Southeastern Bering Sea Cold Pool Area Index Comparisons (NEP10k vs AFSC bottom trawls) for Different Temperature Threshold Definitions					
$\leq 2^\circ\text{C}$		0.853	0.983	1.055	0.865
$\leq 1^\circ\text{C}$		0.885	0.974	0.899	1.050
$\leq 0^\circ\text{C}$		0.563	0.912	0.705	1.311
$\leq -1^\circ\text{C}$		-0.013	0.650	0.343	1.688
Figure 24: CCS Upwelling Indice Timeseries (NEP10k vs CUTI) at Different Latitudes					
45N		0.726	0.874	1.098	1.222
42N		0.837	0.890	0.945	0.894
39N		0.508	0.832	0.763	1.397
36N		0.745	0.785	1.021	1.136
33N		0.248	0.525	0.760	1.532

**Figure S1. Alternative Projection for Figure 1**

As in Figure 1 but using a plate carrée projection for consistency with other mapped figures. The 500m isobath is similarly indicated in dark green.

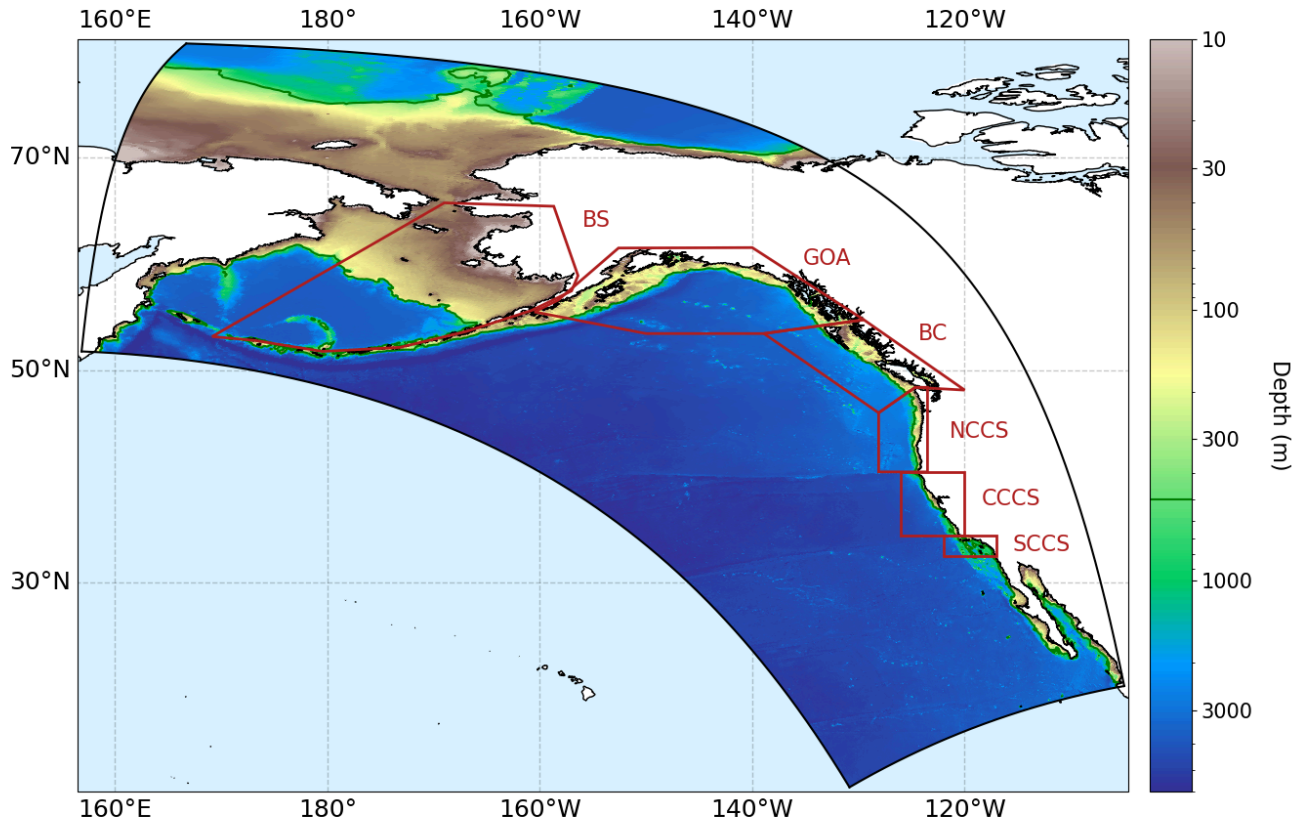


## Figure S2. Extents of Regional Shelves

As in Figure 1 but with bathymetry values only shown inside the regional polygon and where there the shelf criteria is met (i.e., depth  $\leq 500\text{m}$ ). We report both the number of grid cells and total area included in this shelf criteria. We also include transects (blue) showing longer and shorter extents of each shelf (where the shorter dimension is at least one gridcell in length)

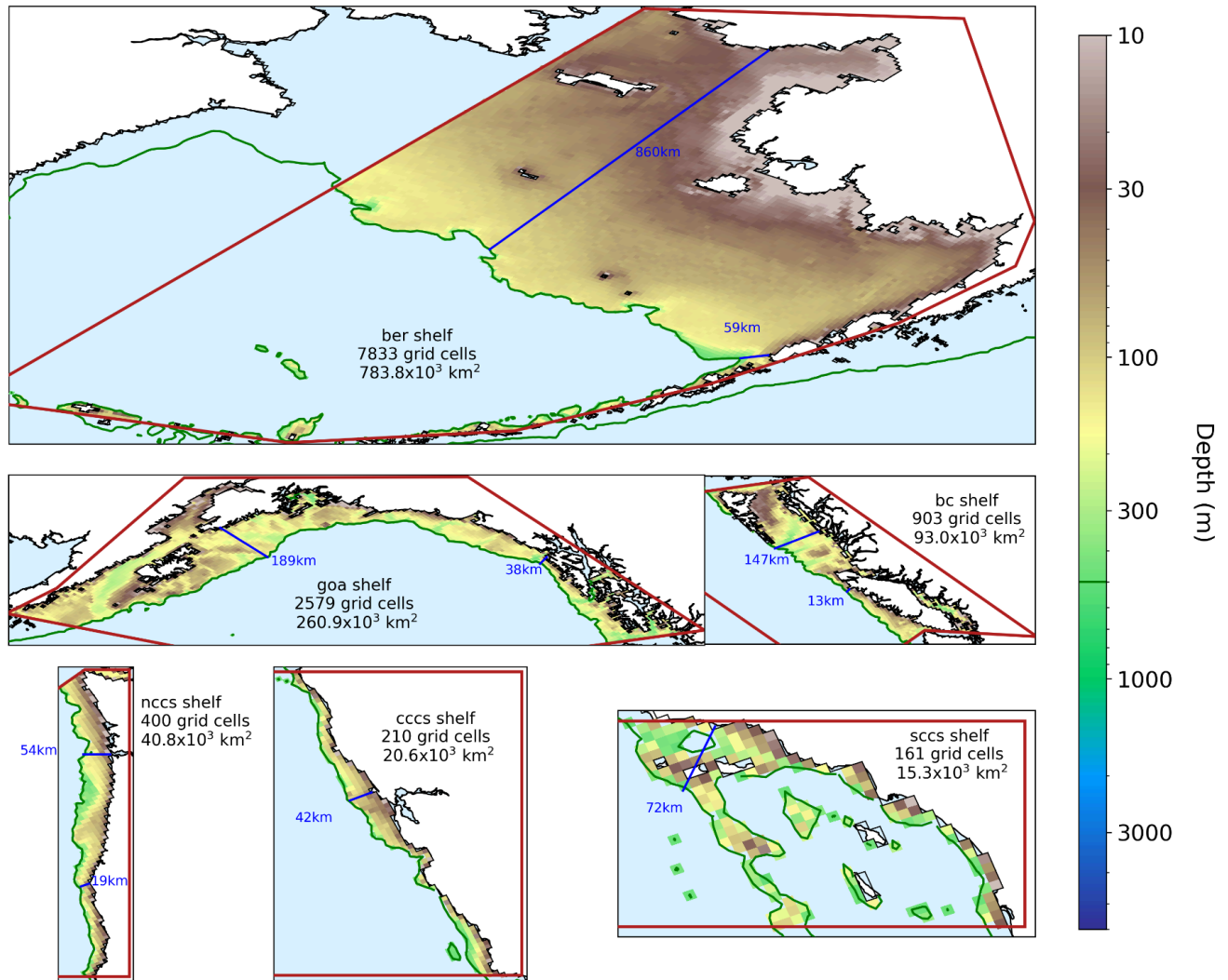


### Figure S3. Spinup Anomaly Timeseries

Monthly anomaly timeseries from the model spinup simulation for shelf surface and bottom temperature and salinity, surface nitrate, and bottom oxygen for the regions outlined in Figure 1. The dashed line indicates the 10 year point when we launch the hindcast simulation evaluated in the main text. Note: we only initialize the model with the biogeochemical conditions from the spinup. Temperature and Salinity are shown here for illustrative purposes.

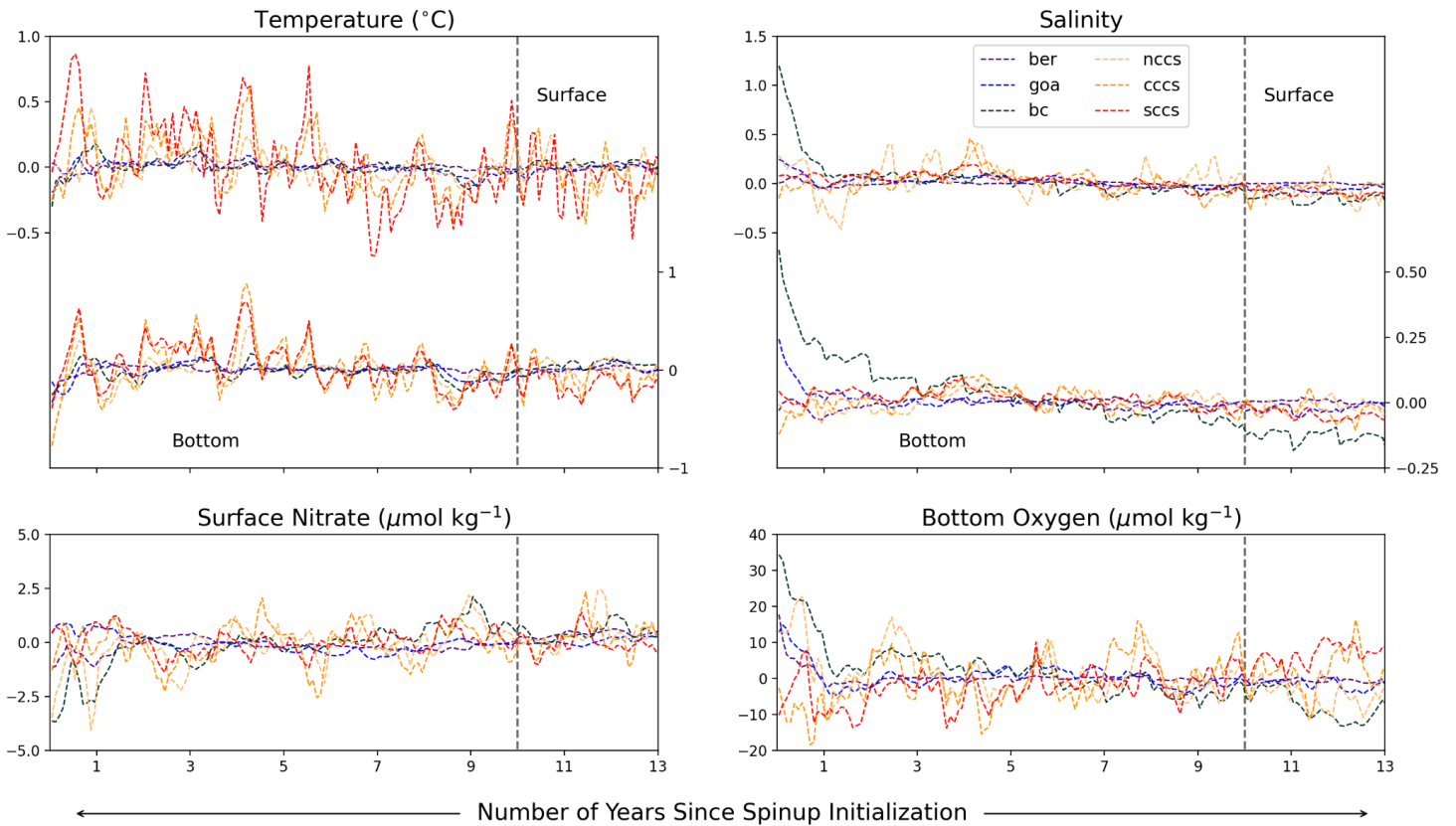


### Figure S4. Ocean Winter (JFM) Temperature for 1993-2019

As in Figure 2 but for 3-month (January-February-March) climatological winter

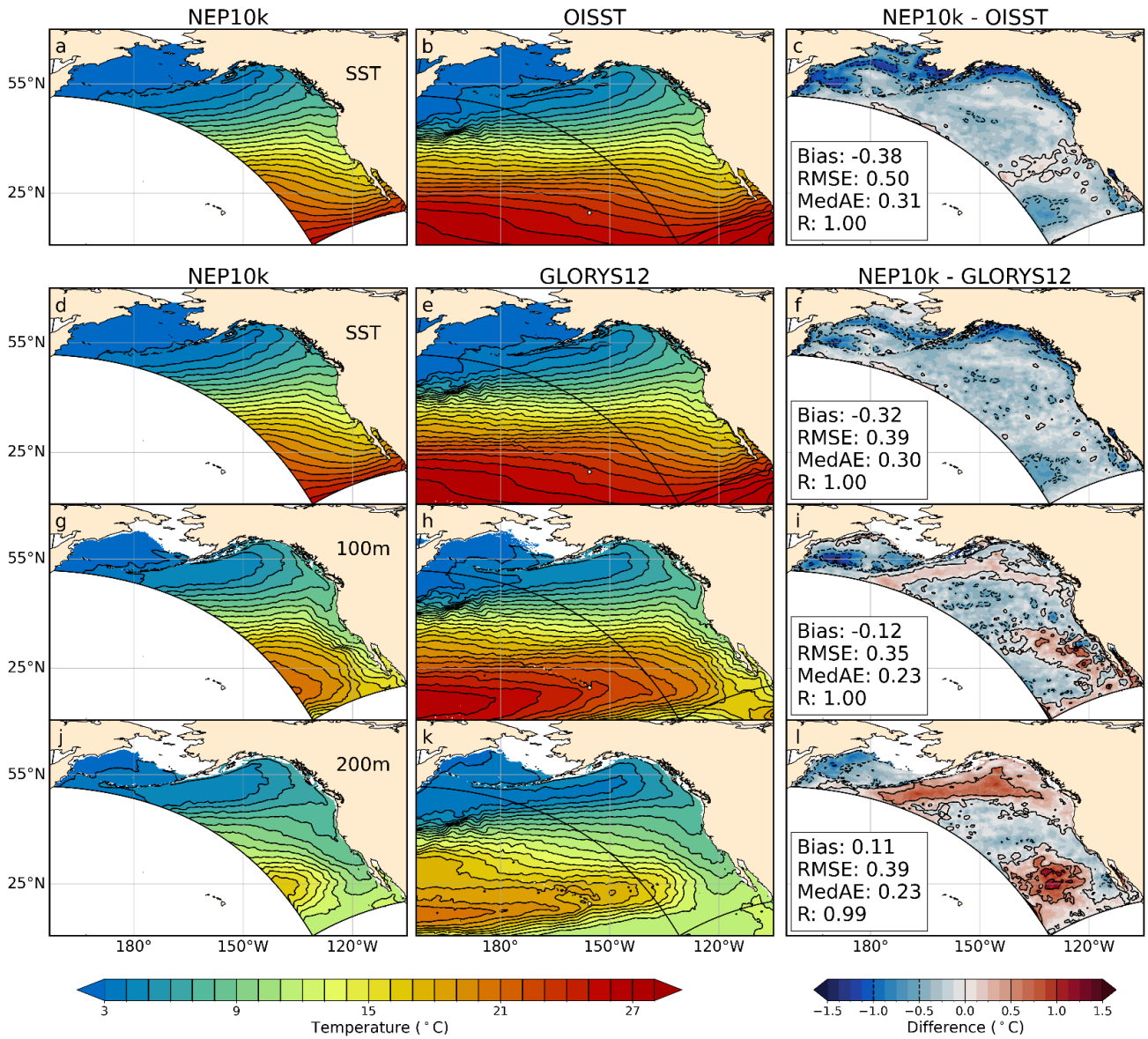


### Figure S5. Ocean Summer (JAS) Temperature for 1993-2019

As in Figure 2 but for 3-month (July-August-September) climatological summer

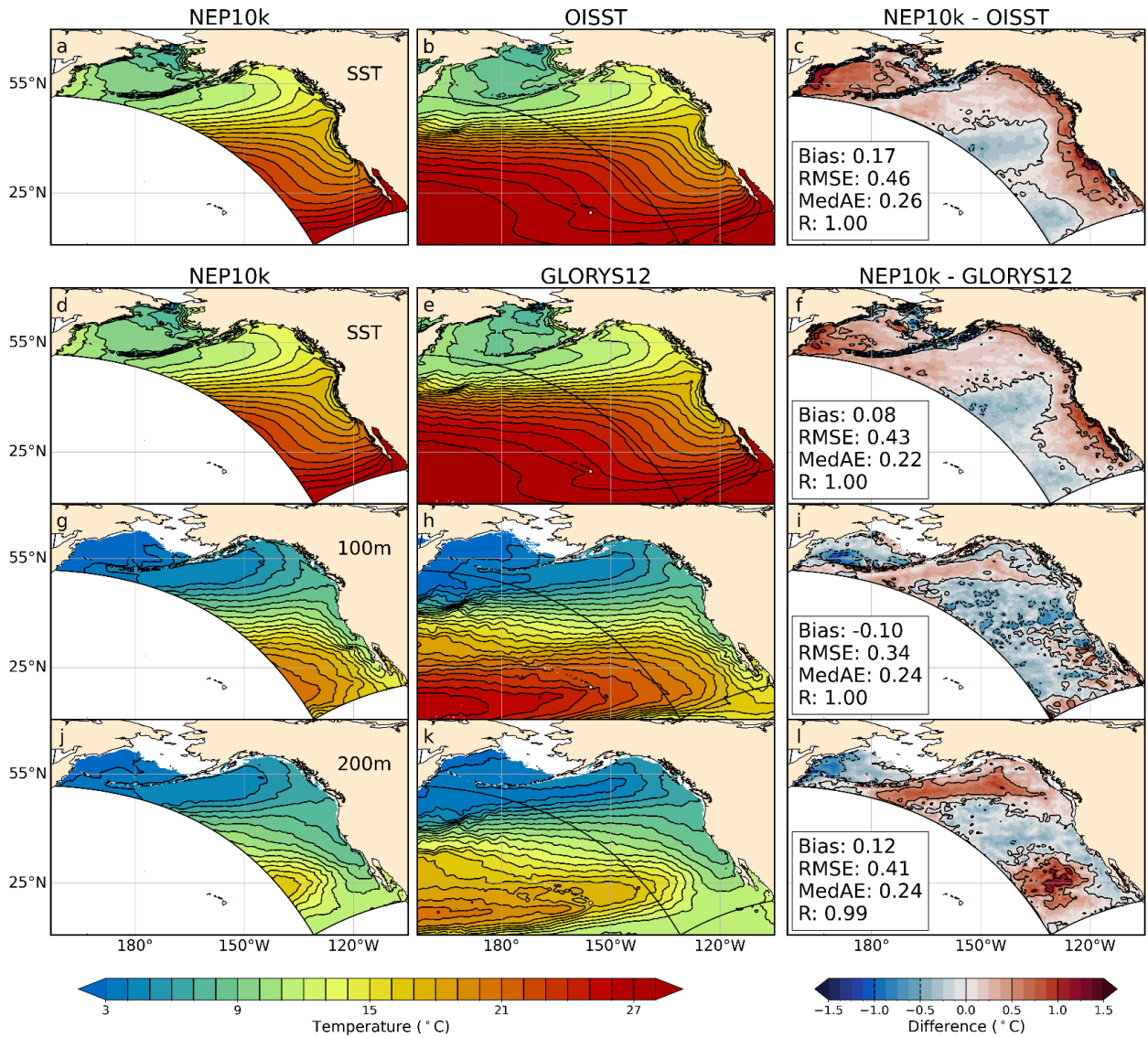


### Figure S6. Winter (JFM) Ocean Salinity

As in Figure 3 but for 3-month (January-February-March) climatological winter

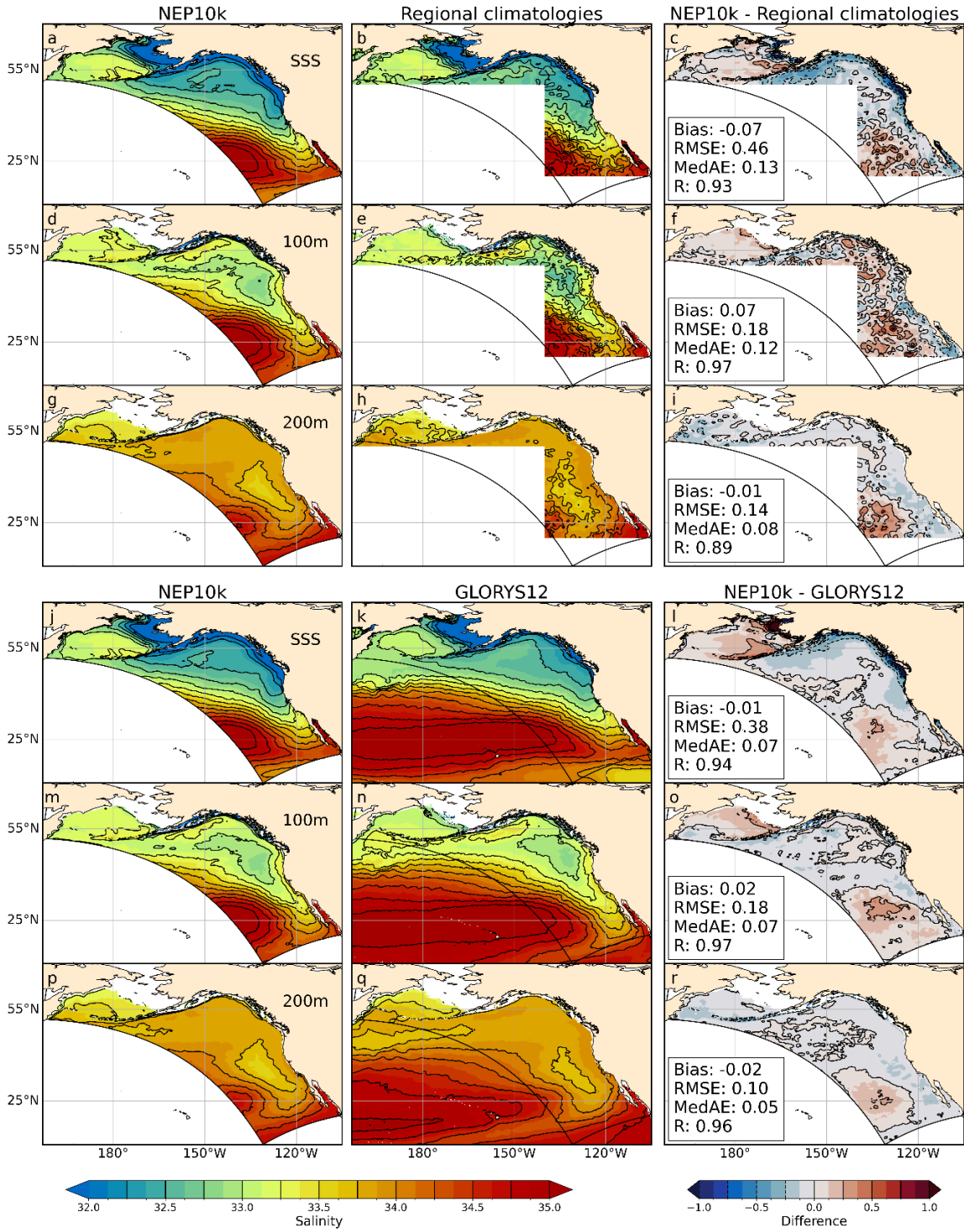




### Figure S7. Summer (JAS) Ocean Salinity

As in Figure 3 but for 3-month (July-August-September) climatological summer

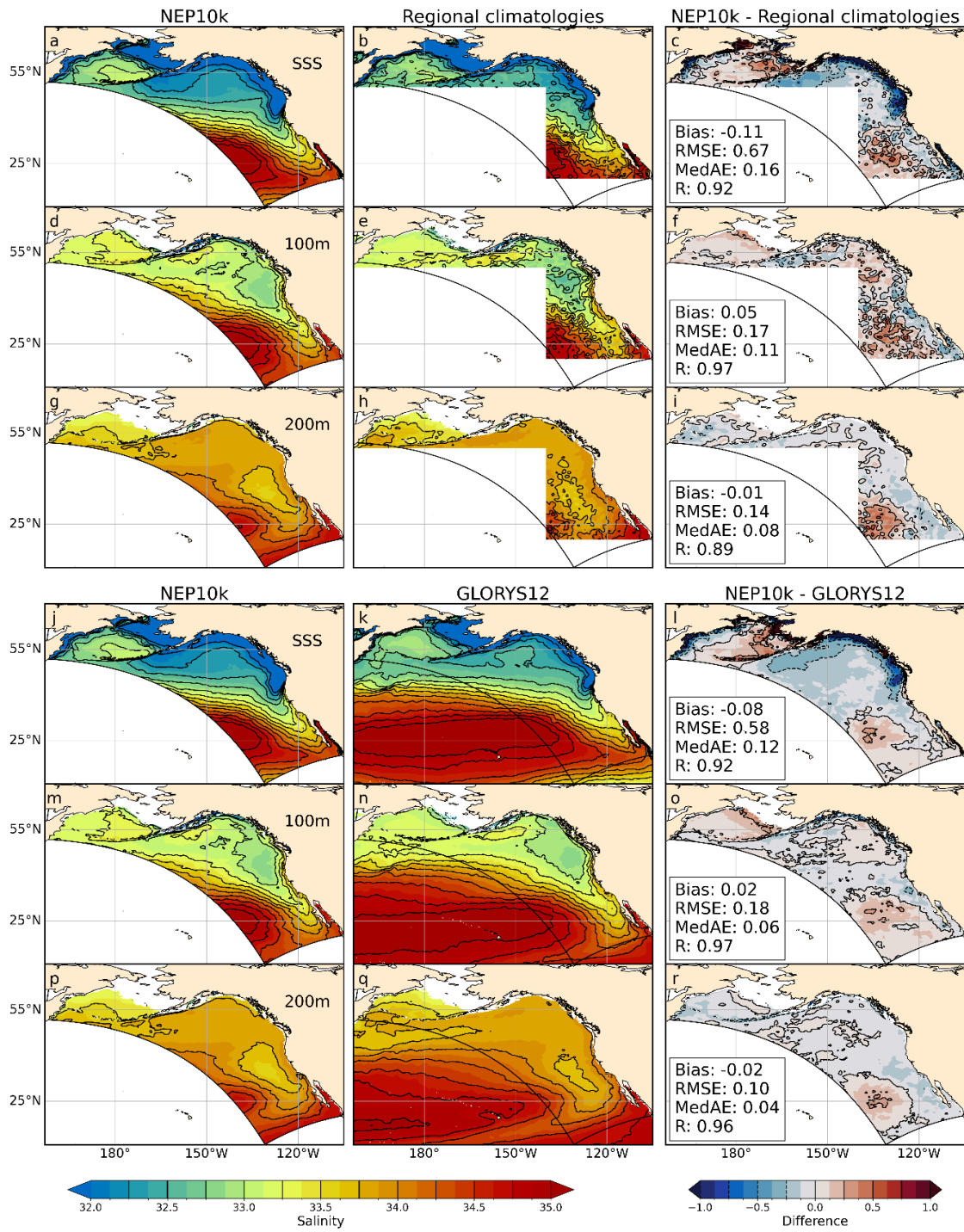


### Figure S8. Winter (JFM) Mixed Layer Depth

As in Figure 4 but for 3-month (January-February-March) climatological winter

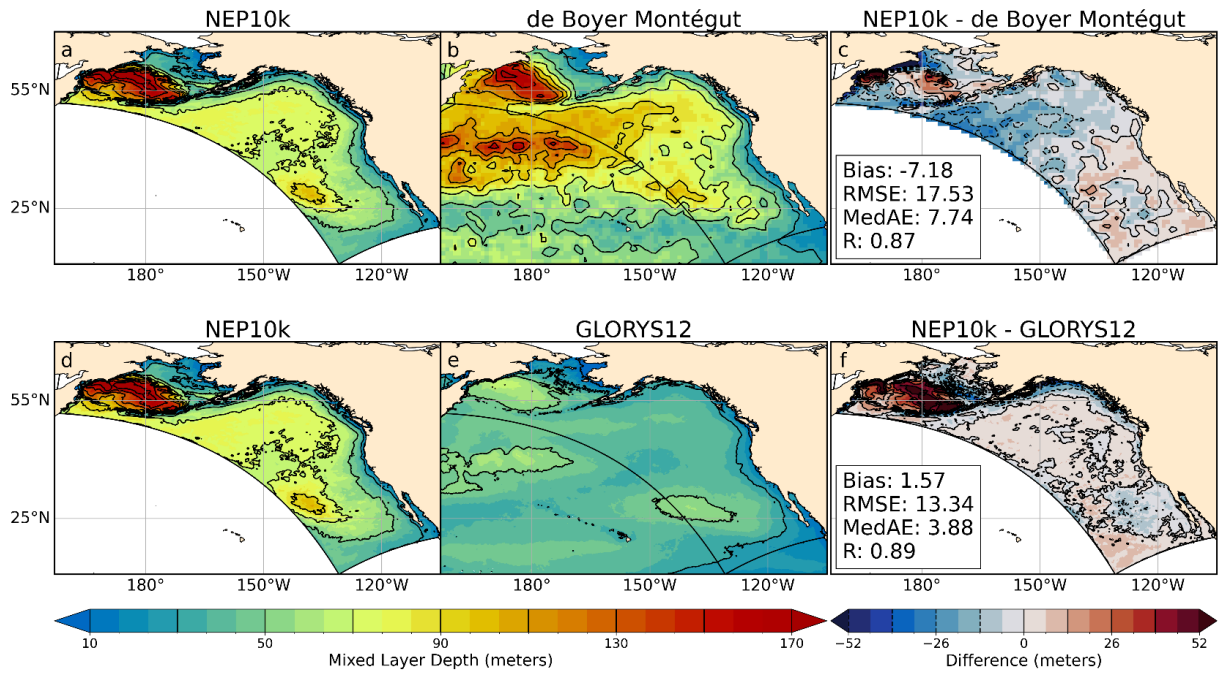


### Figure S9. Summer (JAS) Mixed Layer Depth

As in Figure 4 but for 3-month (July-August-September) climatological summer

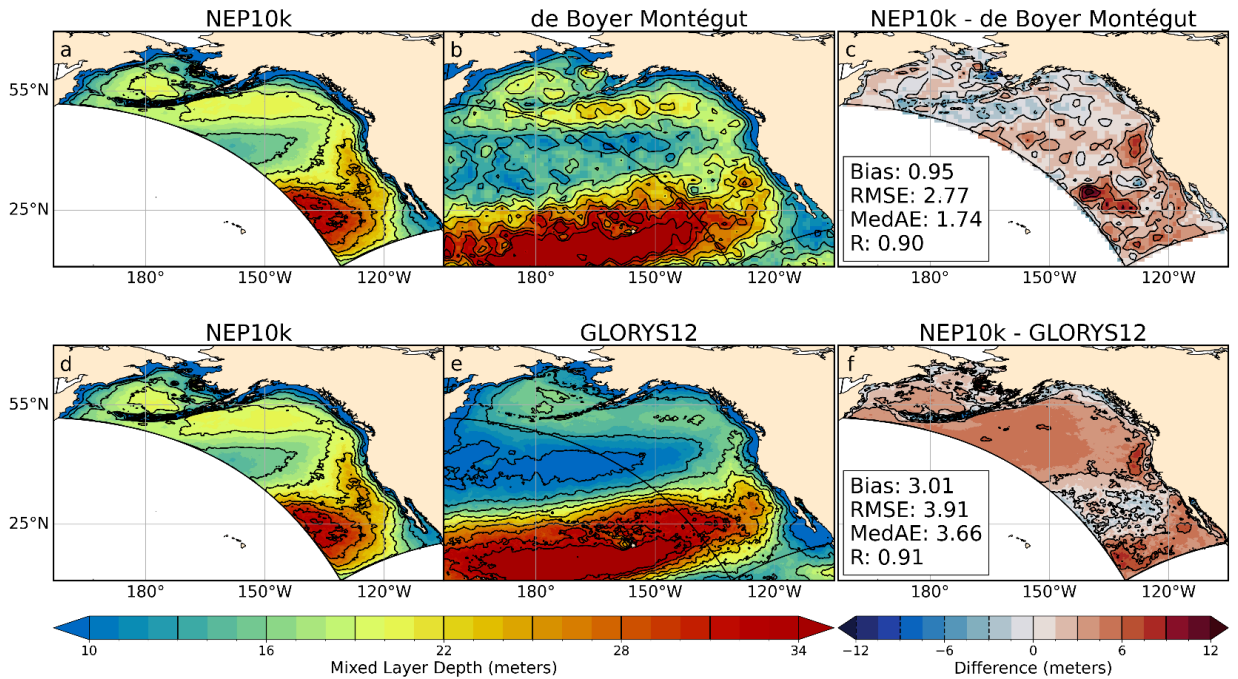


### Figure S10. Winter (JFM) sea surface height comparison

As in Figure 5 but for 3-month (January-February-March) climatological winter

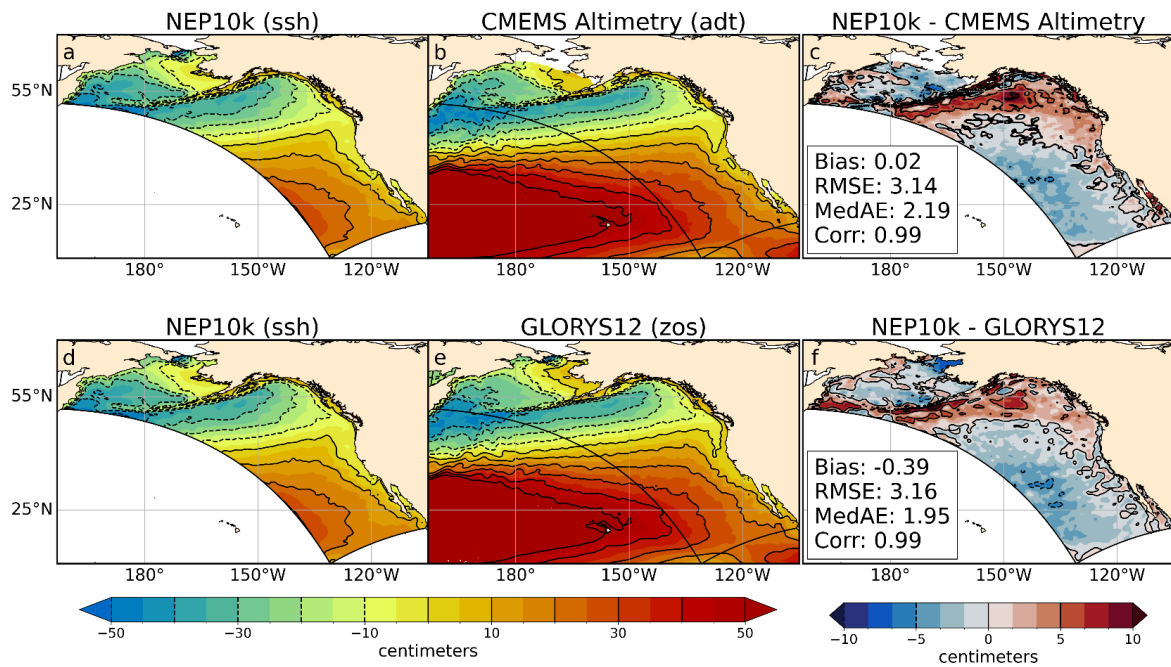


### Figure S11. Summer (JAS) sea surface height comparison

As in Figure 5 but for 3-month (July-August-September) climatological summer

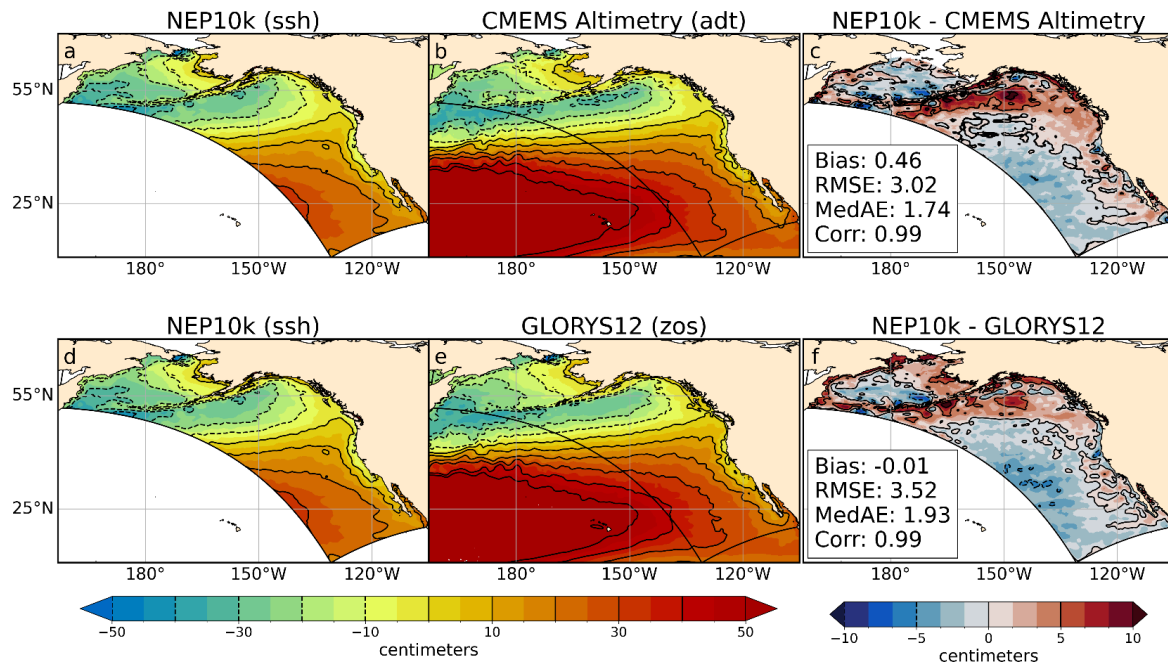


### Figure S12. Tidal Analyses in the Eastern Bering Sea and Western Gulf of Alaska

Same as in Figure 6 but focused specifically in the eastern Bering Sea and western Gulf of Alaska to further inspect inconsistencies between TPXO and NEP10k

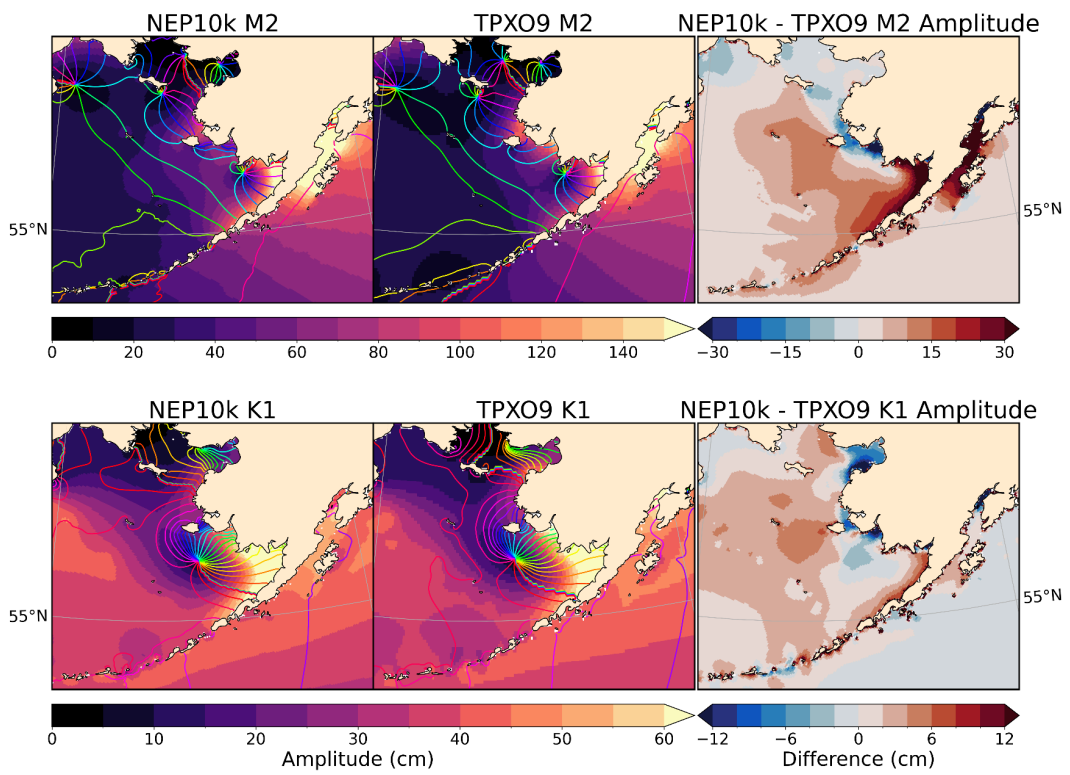


### Figure S13. Tide Gauge Comparisons

We compared the NEP10k and TPXO tidal harmonic constituents against NOAA tide gauges

(<https://tidesandcurrents.noaa.gov/>) in the Gulf of Alaska and Bering Sea (gauge locations in map, right). Using a nearest source-to-destination xesmf regridding, we selected the NEP10k and TPXO ocean gridcell closest to each tide gauge and plot the constituent (M2, K1) amplitude and phase at these locations against the same values calculated for the corresponding tide gauges; we report the statistics from these 16 points and plot a dashed 1-to-1 line for reference. We also show several maps (bottom) depicting a subset of tide gauge locations (low opacity) relative to the ocean grid cell (smaller; high opacity) selected for NEP10k and TPXO comparisons in the context of each product's land mask (outline in dark blue; Cartopy land mask included in beige for reference). These maps illustrate the models' coarse approximation of complex coastal geometry that could impact model reproduction of tidal signals near the coast.

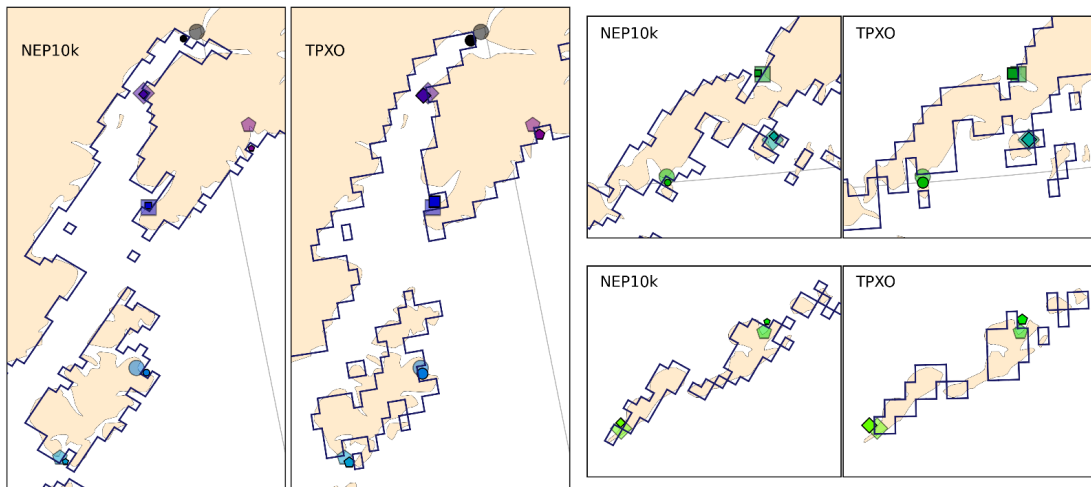
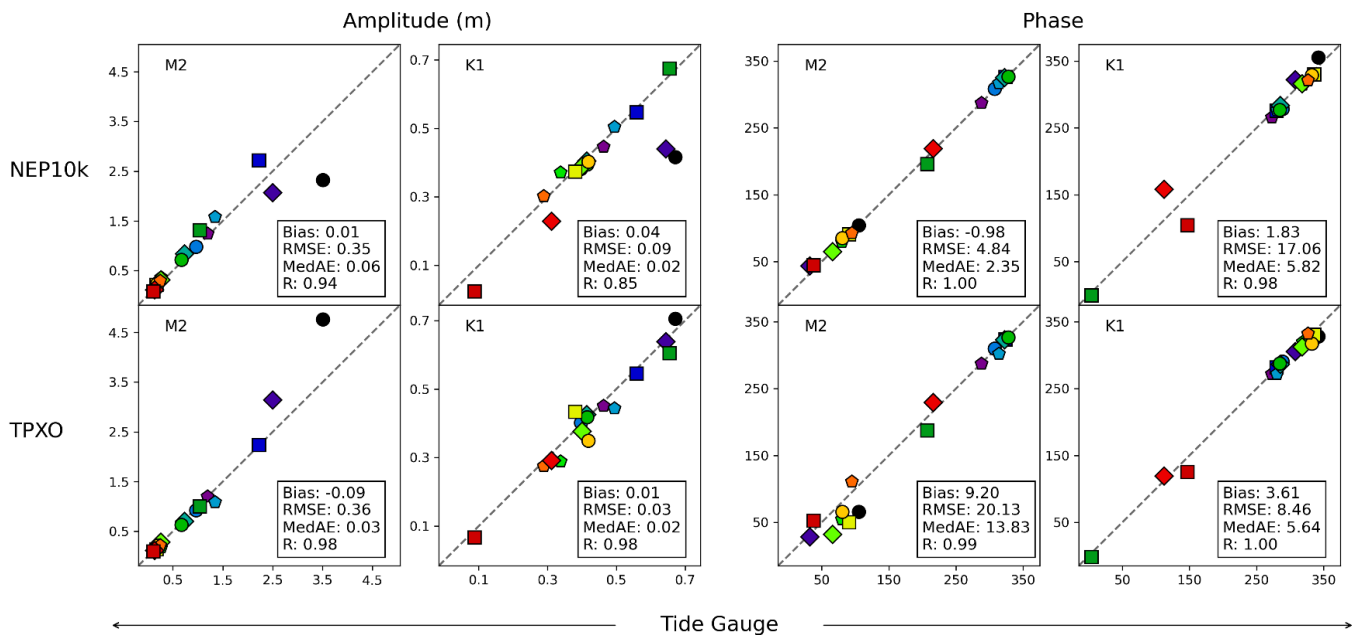
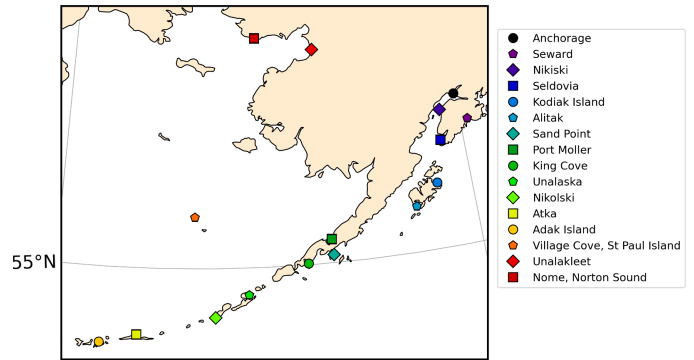


### Figure S14. Winter (JFM) Nitrate Concentration

As in Figure 7 but for 3-month (January-February-March) climatological winter

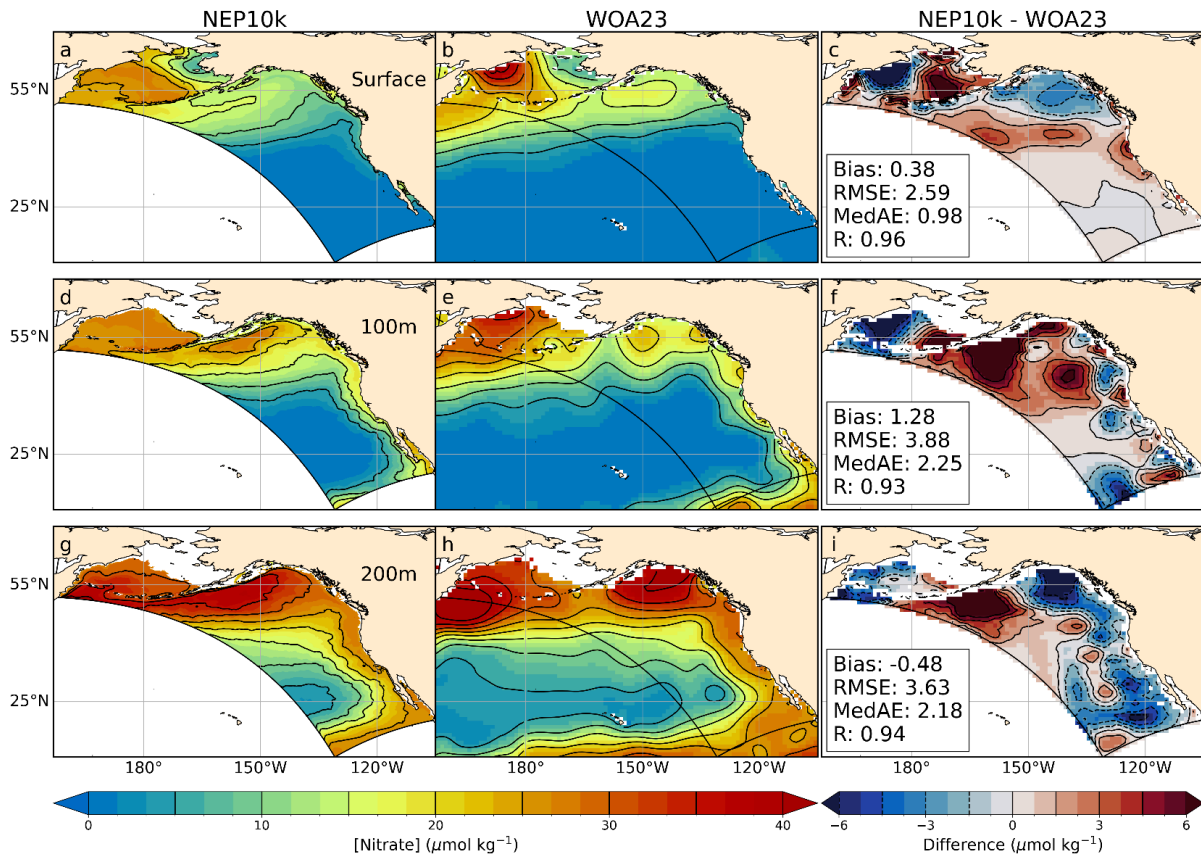


### Figure S15. Summer (JAS) Nitrate Concentration

As in Figure 7 but for 3-month (July-August-September) climatological summer

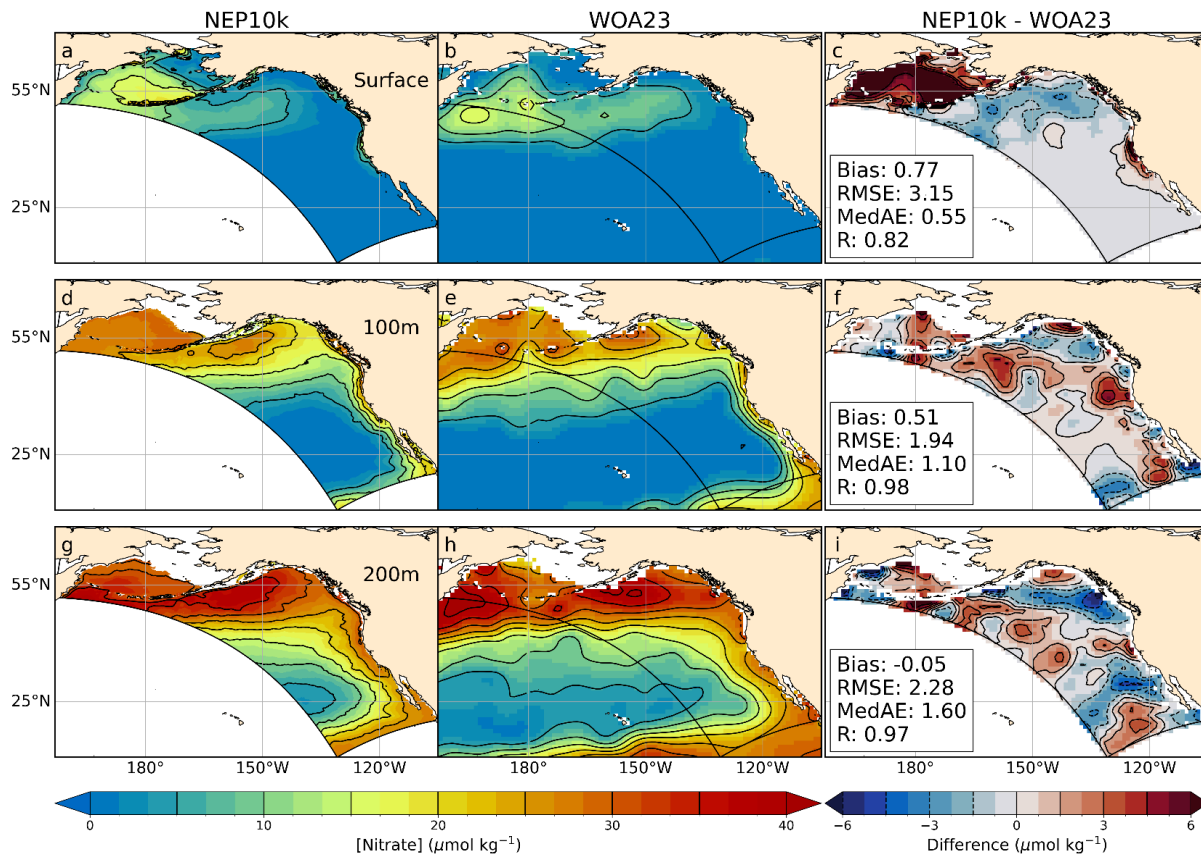


### Figure S16. Winter (JFM) Phosphate Concentration

As in Figure 8 but for 3-month (January-February-March) climatological winter

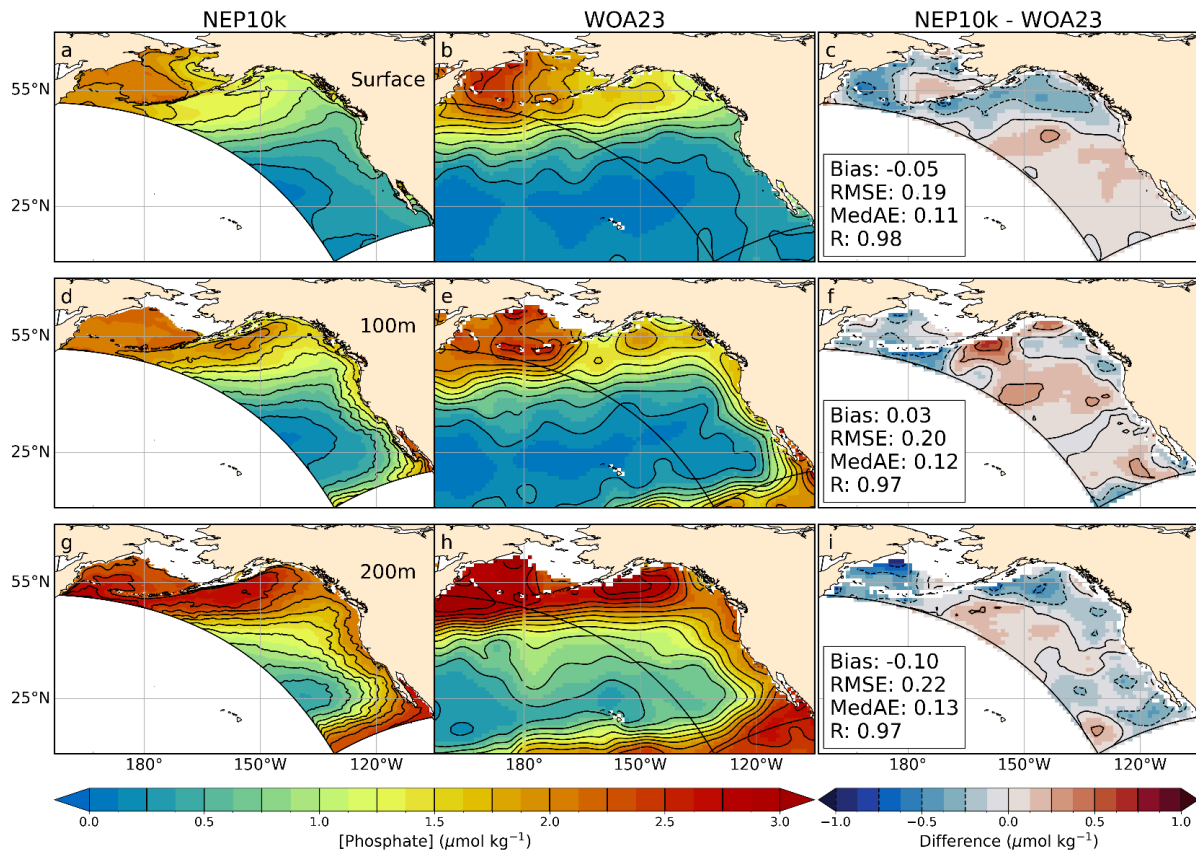




### Figure S17. Summer (JAS) Phosphate Concentration

As in Figure 8 but for 3-month (July-August-September) climatological summer

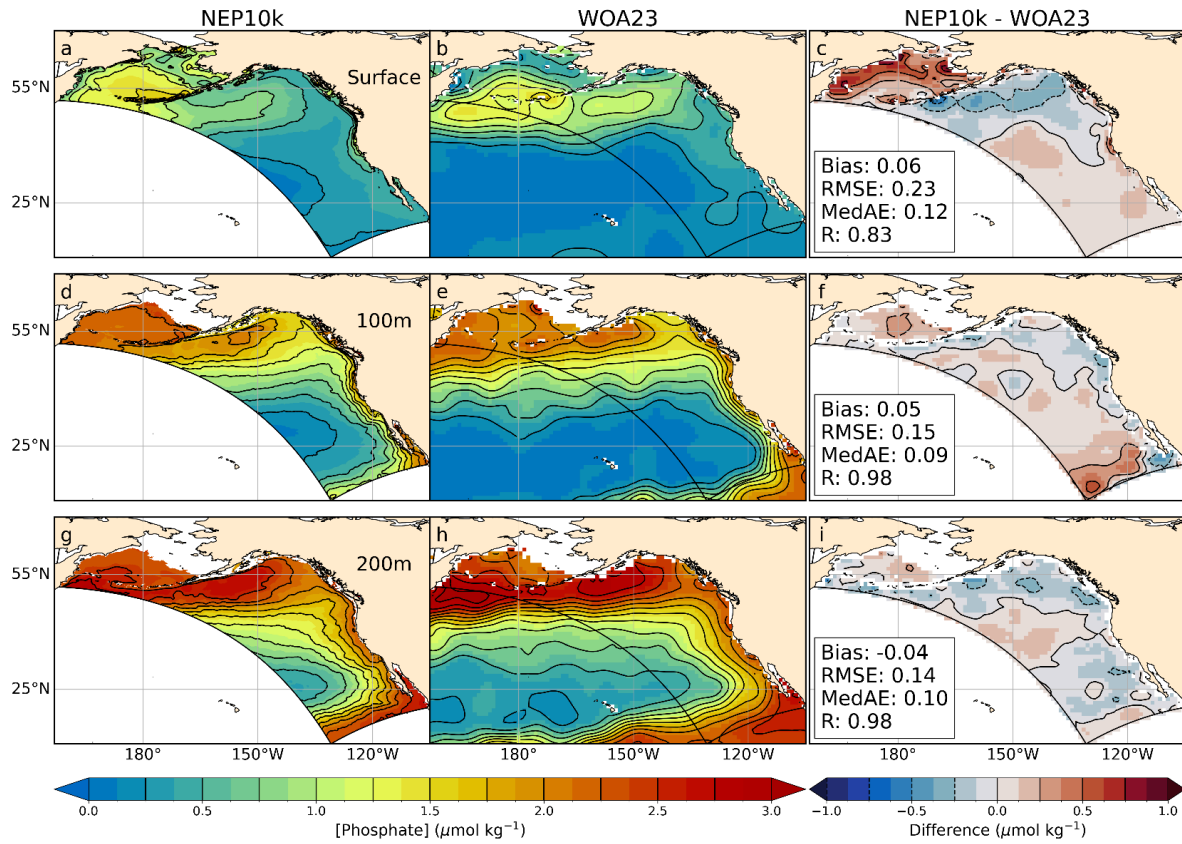


### Figure S18. Seasonal Surface Dissolved Iron Concentration and Primary Phytoplankton Nutrient Limitations

As in Figure 9 but for 3-month climatological seasonal means for Winter (Jan-Feb-Mar), Spring (Apr-May-Jun), Summer (July-Aug-Sept), and Winter (Oct-Nov-Dec).

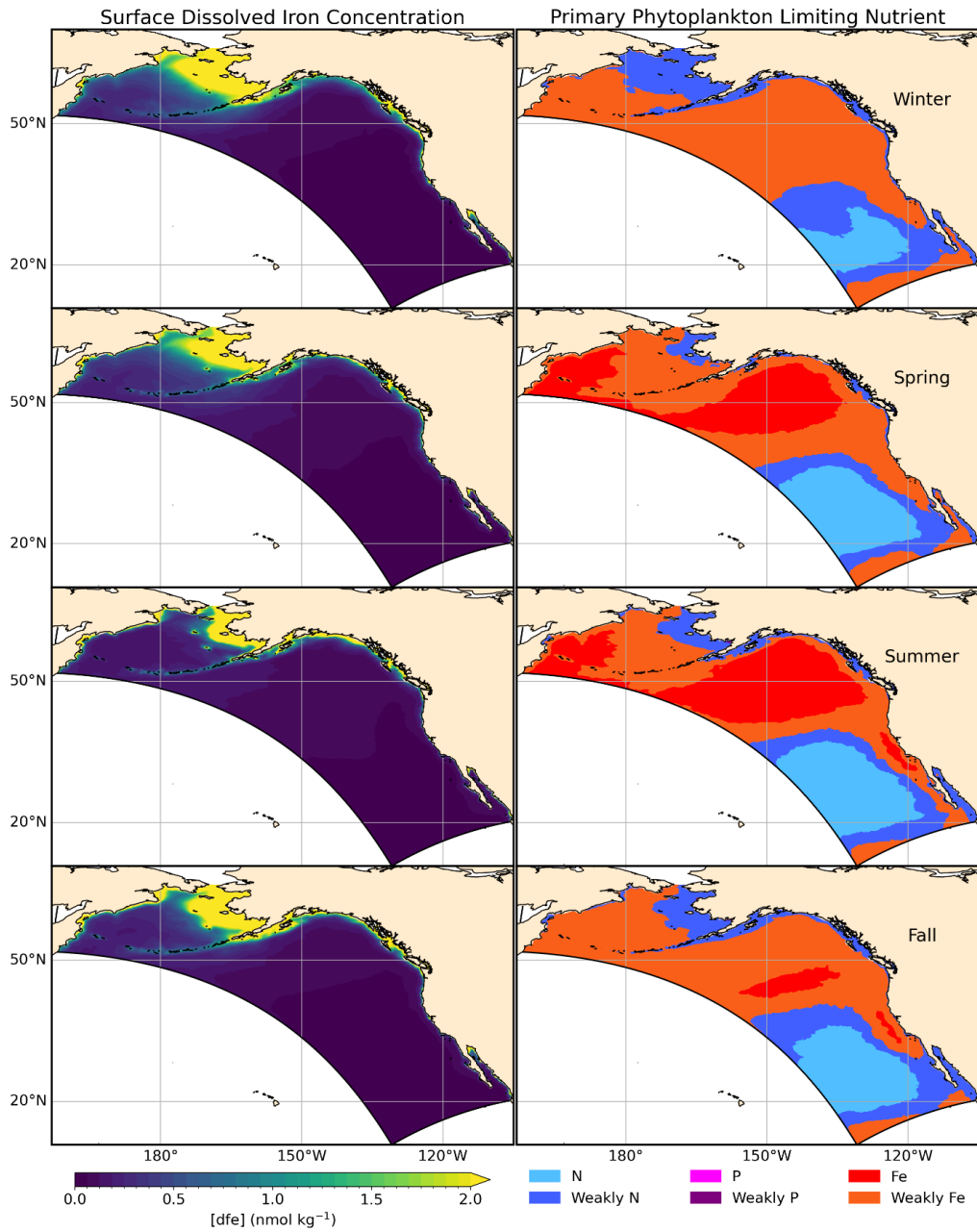


### Figure S19. Winter (JFM) Oxygen Concentration

As in Figure 12 but for 3-month (January-February-March) climatological winter

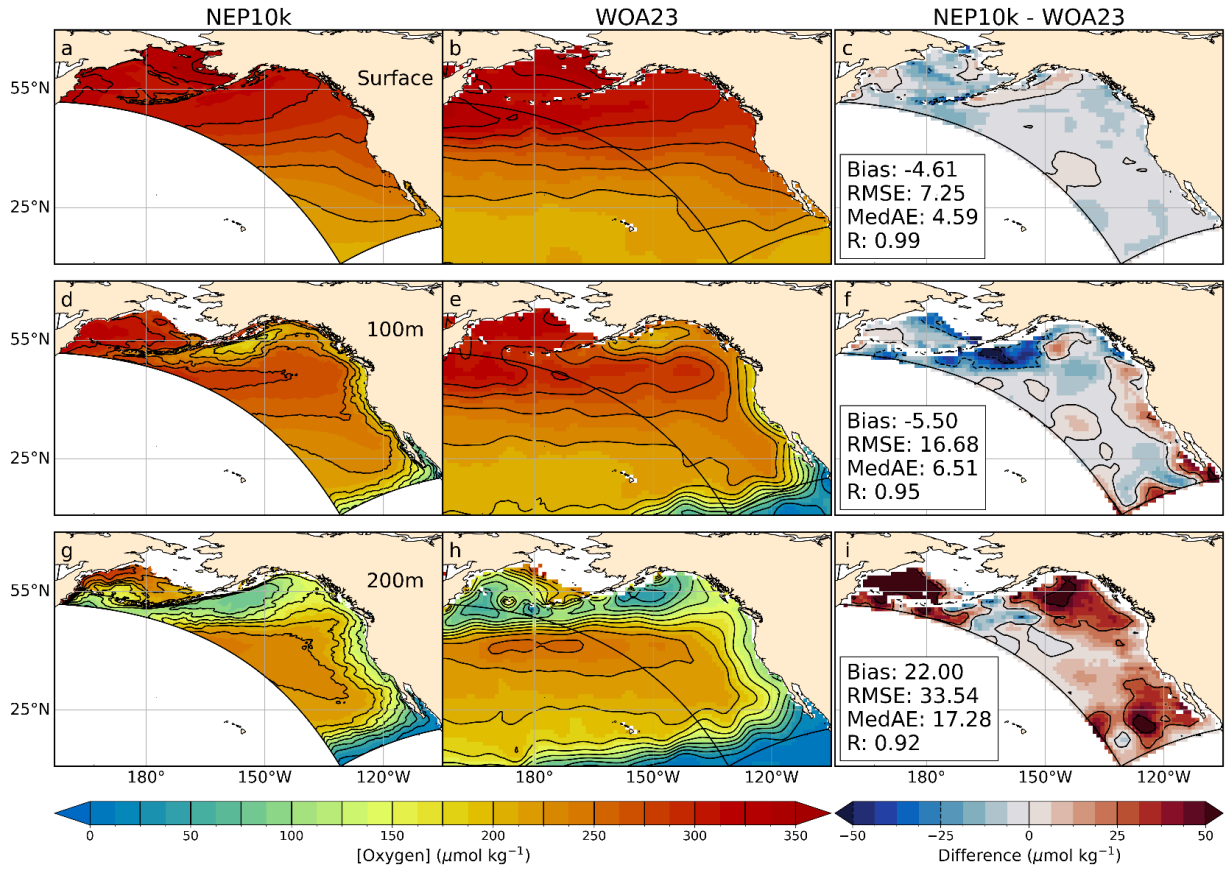


### Figure S20. Sumer (JAS) Oxygen Concentration

As in Figure 12 but for 3-month (July-August-September) climatological summer

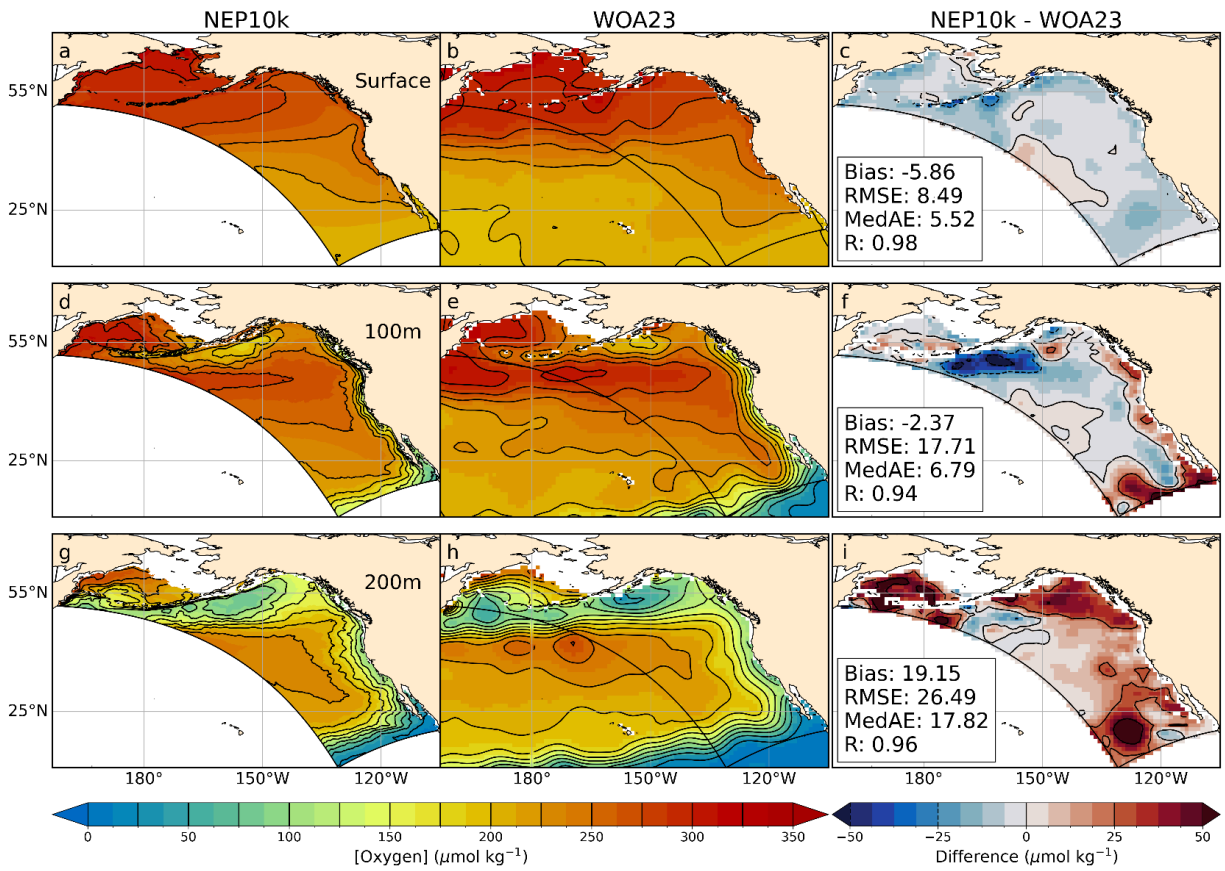


### Figure S21. Bering Sea Ice Extent Timeseries

Comparisons of Total area of the South Eastern Bering Sea (Rohan et al., 2022) exhibiting sea ice concentrations of 15% or greater by month as observed by satellites (black) and simulated by NEP10k (red) .

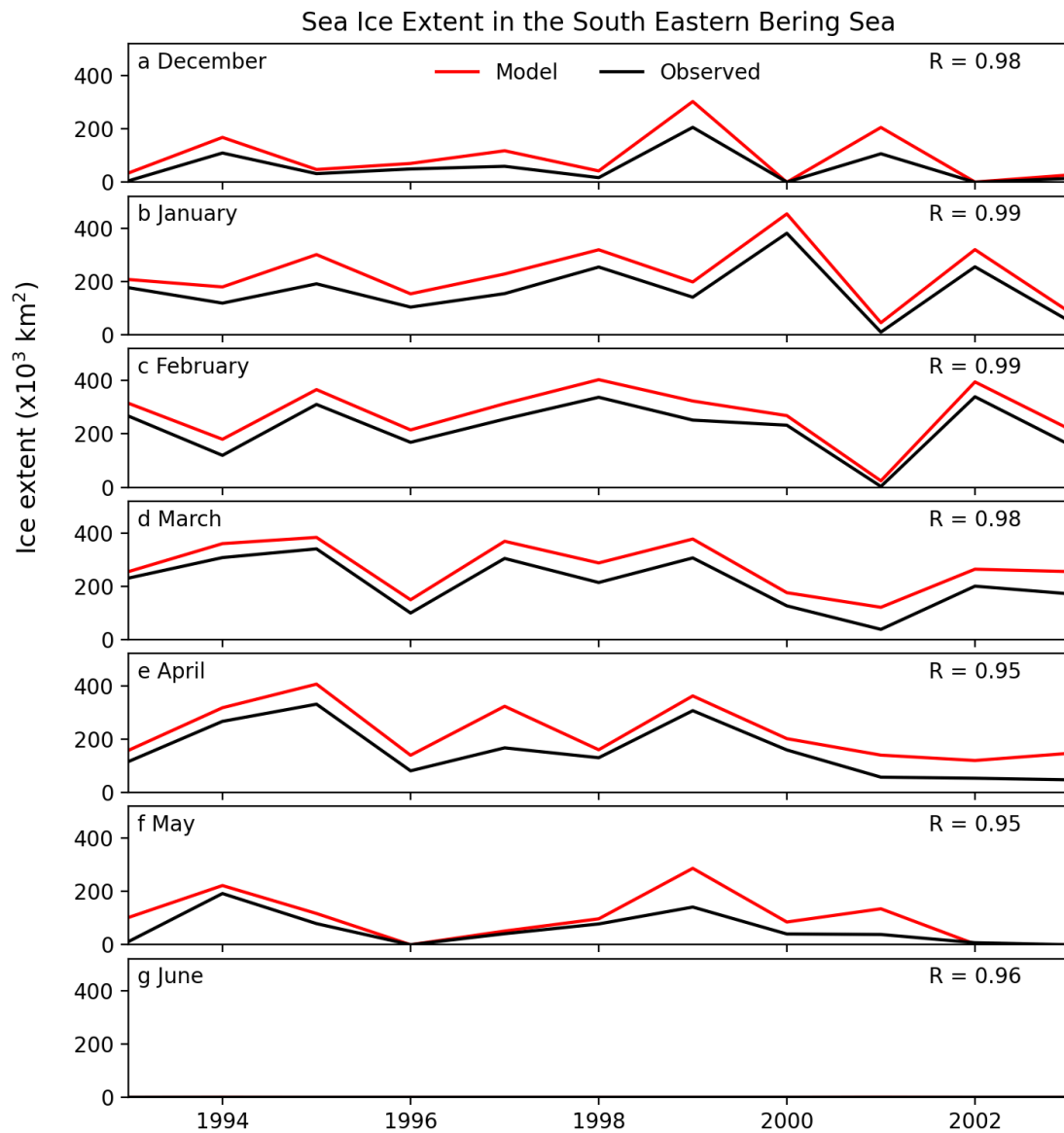


### Figure S22. NGAO Composites

Composites of important ecological conditions during the positive (NGAO >1; 54 months out of 324) and the negative (NGAO < -1; 56 months out of 324) phases of the Gulf of Alaska Downwelling Index (NGAO). Grid cells are colored where the composite differs significantly from 0 (i.e., student t-test,  $p < 0.05$ ).

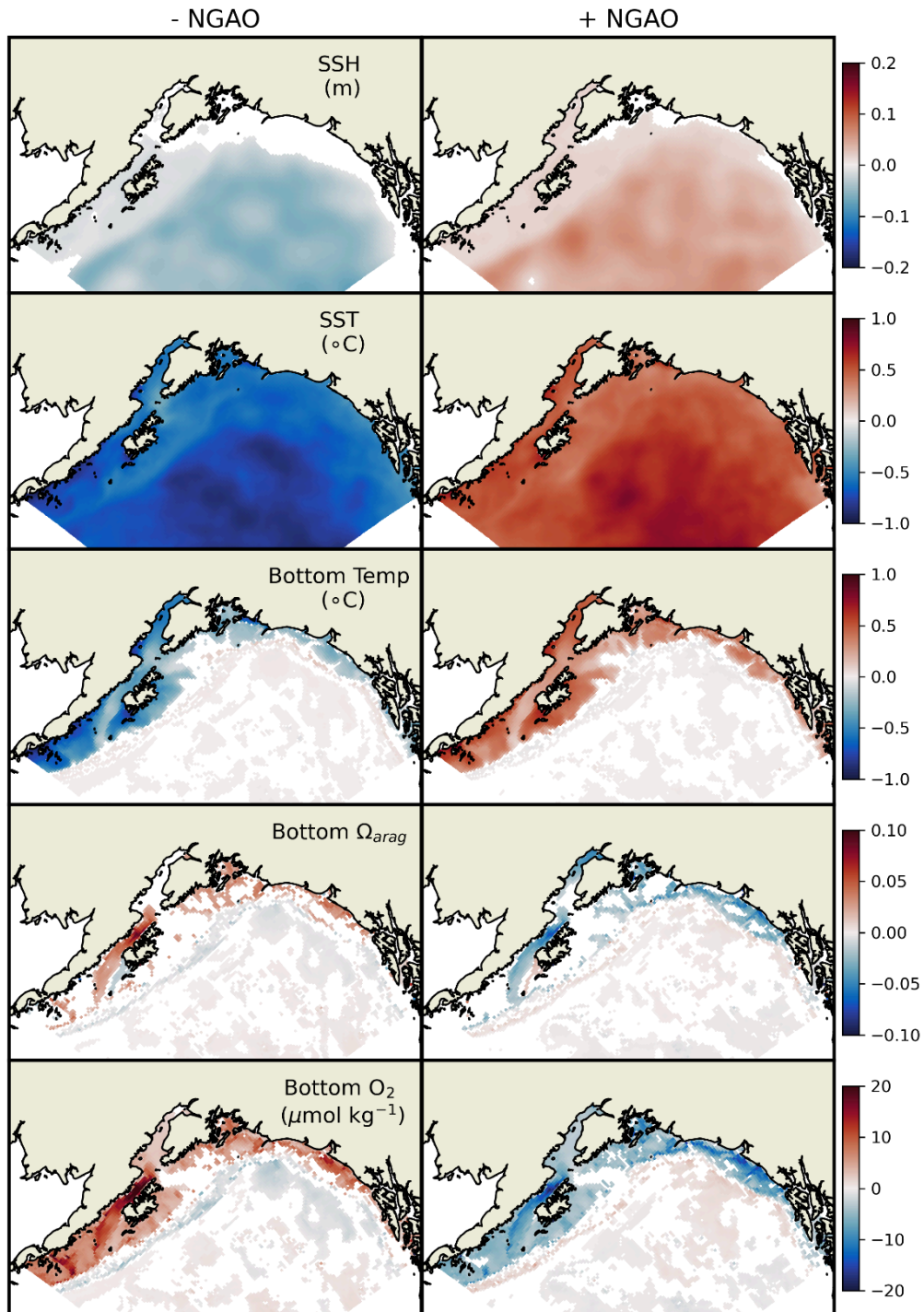


### Figure S23. Annual Mixed Layer Depth Comparisons with NEP10k using Fox-Kemper MLD Restratification

Same as Fig. 4 but with NEP10k using the Fox-Kemper restratification methods as in Ross et al., (2023). However, due to the higher latitudes of the NEP10k domain relative to the NWA domain, we set the submesoscale eddy front length 800m for this sensitivity comparison rather than 1500m used in Ross et al., (2023).

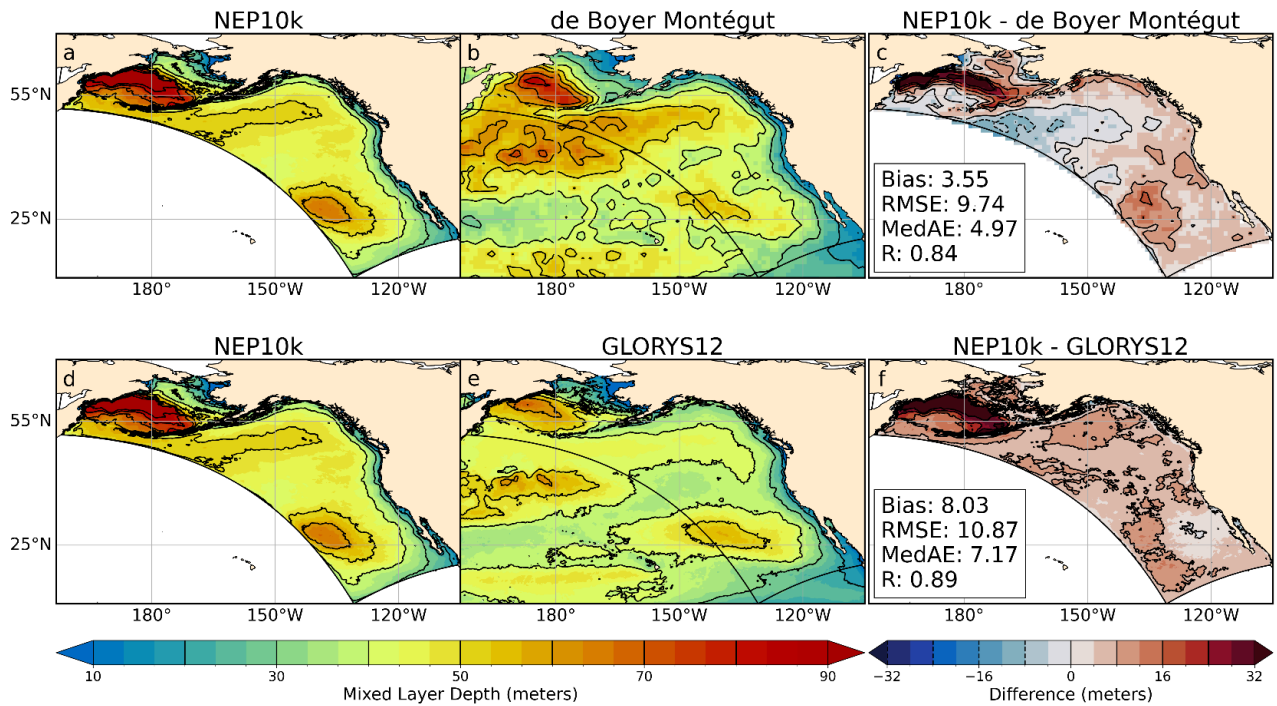


**Figure S24. Timeseries, climatologies and correlations of NEP10k EBS cold pool area index.**

The top plot shows monthly timeseries of the relative area of the Eastern Bering Sea that is covered in bottom water of a temperature less than or equal to the threshold values depicted in Fig. 20 (i.e., lightest blue indicates water  $\leq 2^{\circ}\text{C}$ , darkest blue indicates water  $\leq -1^{\circ}\text{C}$ ). Unlike the NEP10k values in Fig.20, these values are calculated for the monthly mean bottom temperature rather than derived from data points that vary in time and space throughout the summer trawl season. The bottom left plot shows monthly climatological values with standard deviation error bars and the timeframe of the AFSC bottom trawl delimited in red dotted lines. Lastly, the lower right panel depicts the Pearson correlation coefficient calculated for each water temperature threshold comparing the timeseries of values for a given month against the trawl-derived value for that year. We would expect most highly correlated values to fall within the time frame of the bottom trawl. However, values with somewhat higher correlation preceding the trawl may be useful for near-term forecasting efforts.

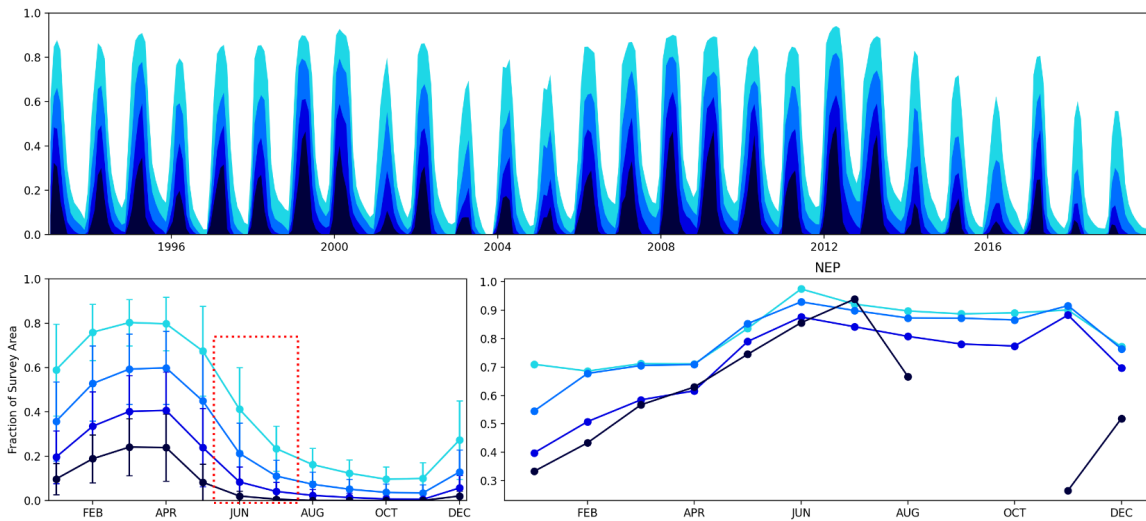




**Figure S25. Difference in monthly climatological sea ice concentration in the SEBS**

The seasonally progressive change in sea concentration within the south eastern Bering Sea where the majority of the Alaska Fisheries Science Center bottom trawl samples are collected. Only declines in monthly sea ice concentration are shown. The Extent of the SEBS is outlined in black (Rohan et al., 2022).

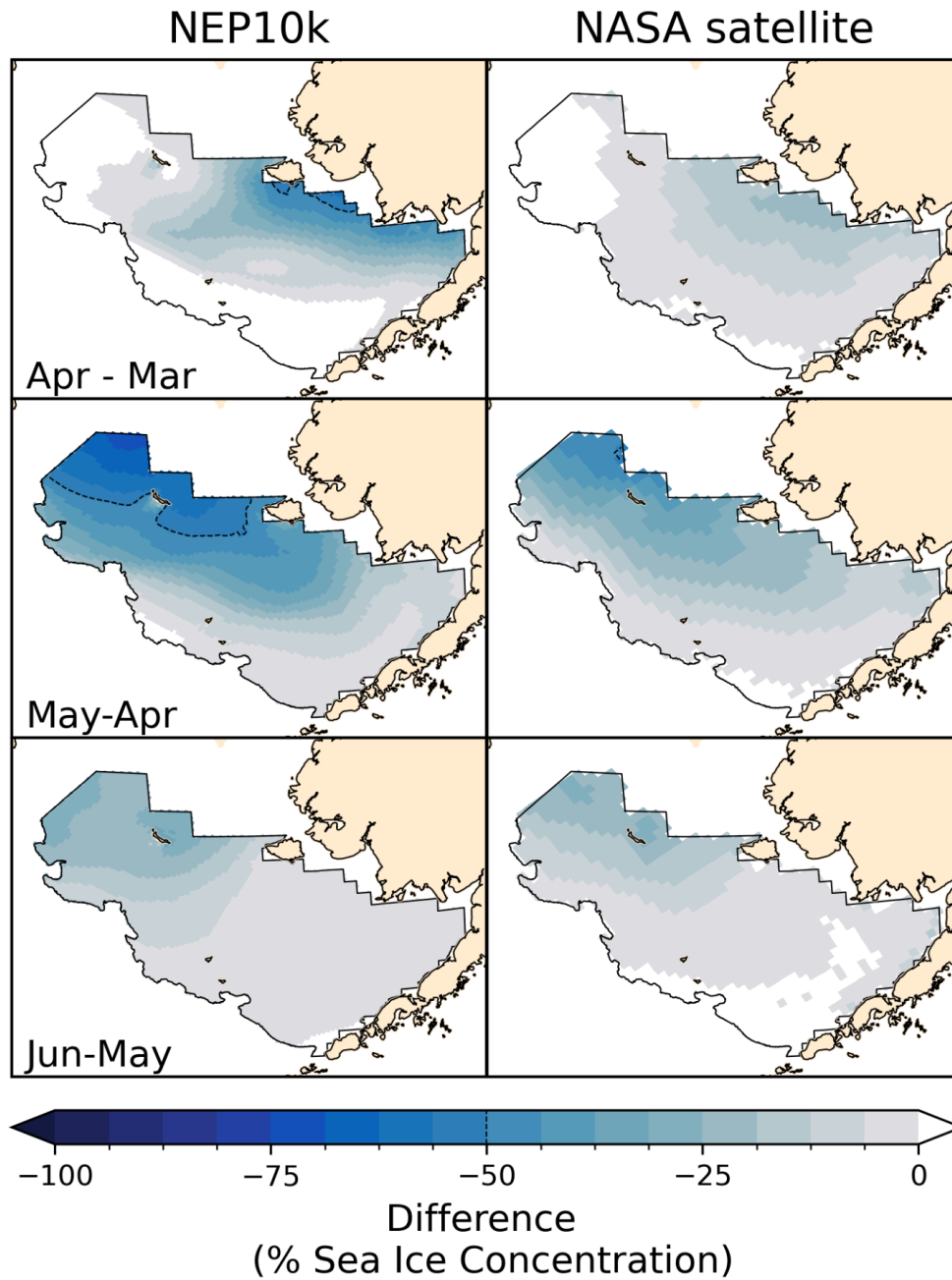


**Figure S26. NEP10k and GLORYS temperature and salinity compared against CalCOFI bottle data 1993-2019**

Monthly NEP10k and daily GLORYS temperature and salinity output were spatially and temporarily regridded to CalCOFI bottle data measurements. Comparisons from all depths and stations are shown below along with the Pearson correlation coefficient and the dashed 1-to-1 line shown for reference.

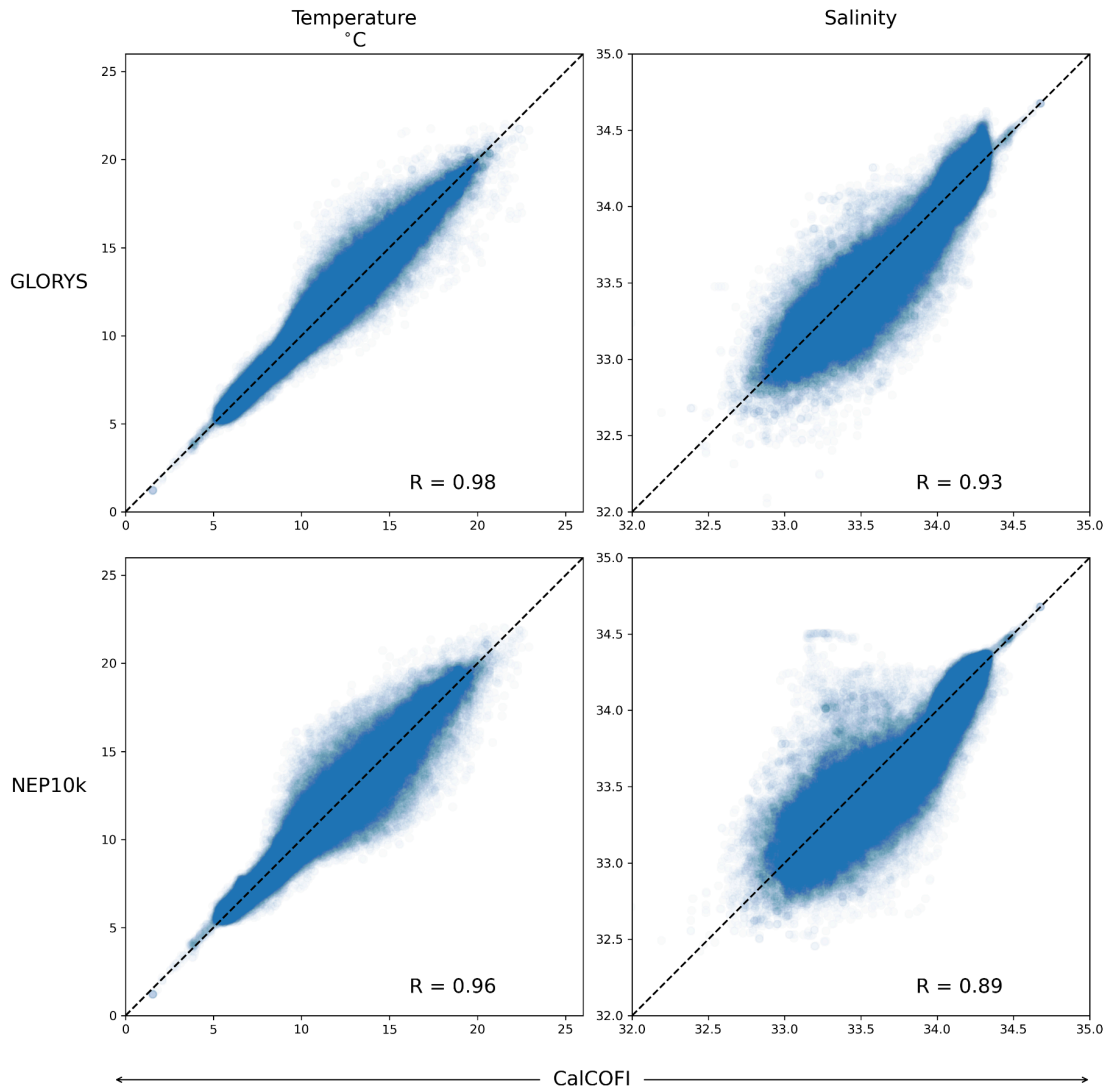


**Figure S27. NEP10k biogeochemistry comparisons against CalCOFI bottle data for** Monthly NEP10k nitrate, oxygen, phosphate, and silicate output were spatially and temporarily regridded to CalCOFI bottle data measurements. Comparisons from all depths and stations are shown below along with the Pearson correlation coefficient and the dashed 1-to-1 line shown for reference.

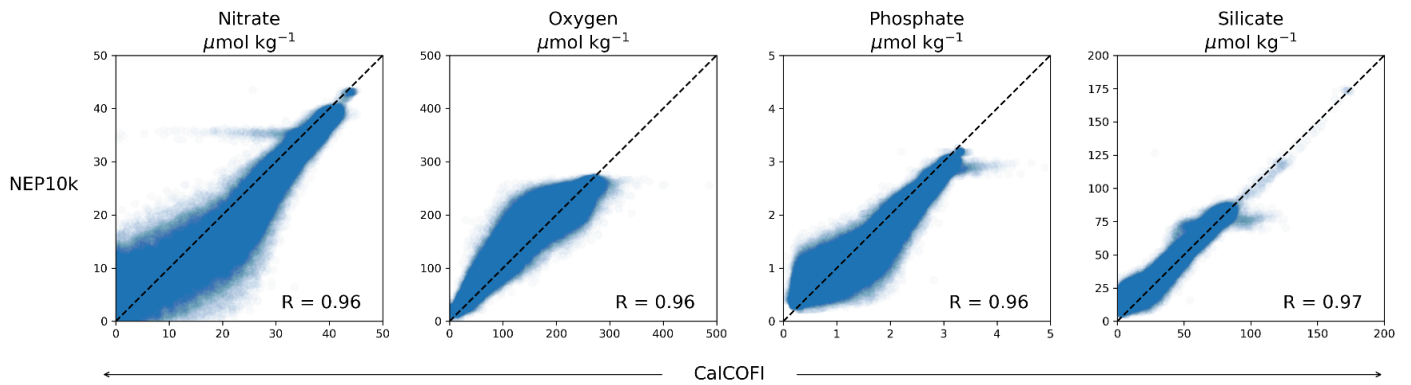


**Figure S28. NEP10k compared against CalCOFI 1993-2019 bottle data**

Taylor diagrams for NEP10k temperature, salinity, nitrate and oxygen compared against CalCOFI bottle data. Normalized standard deviation (standard deviation of the model values divided by that of the CalCOFI data) appears on the x and y axes; Pearson correlation coefficient is expressed as the angle above the x-axis. Each marker indicates a unique station in the CalCOFI array with stations in the same line sharing marker shape and color. Warmer marker colors (e.g., red) indicate stations in more southerly CalCOFI lines (e.g., Line 93.3)

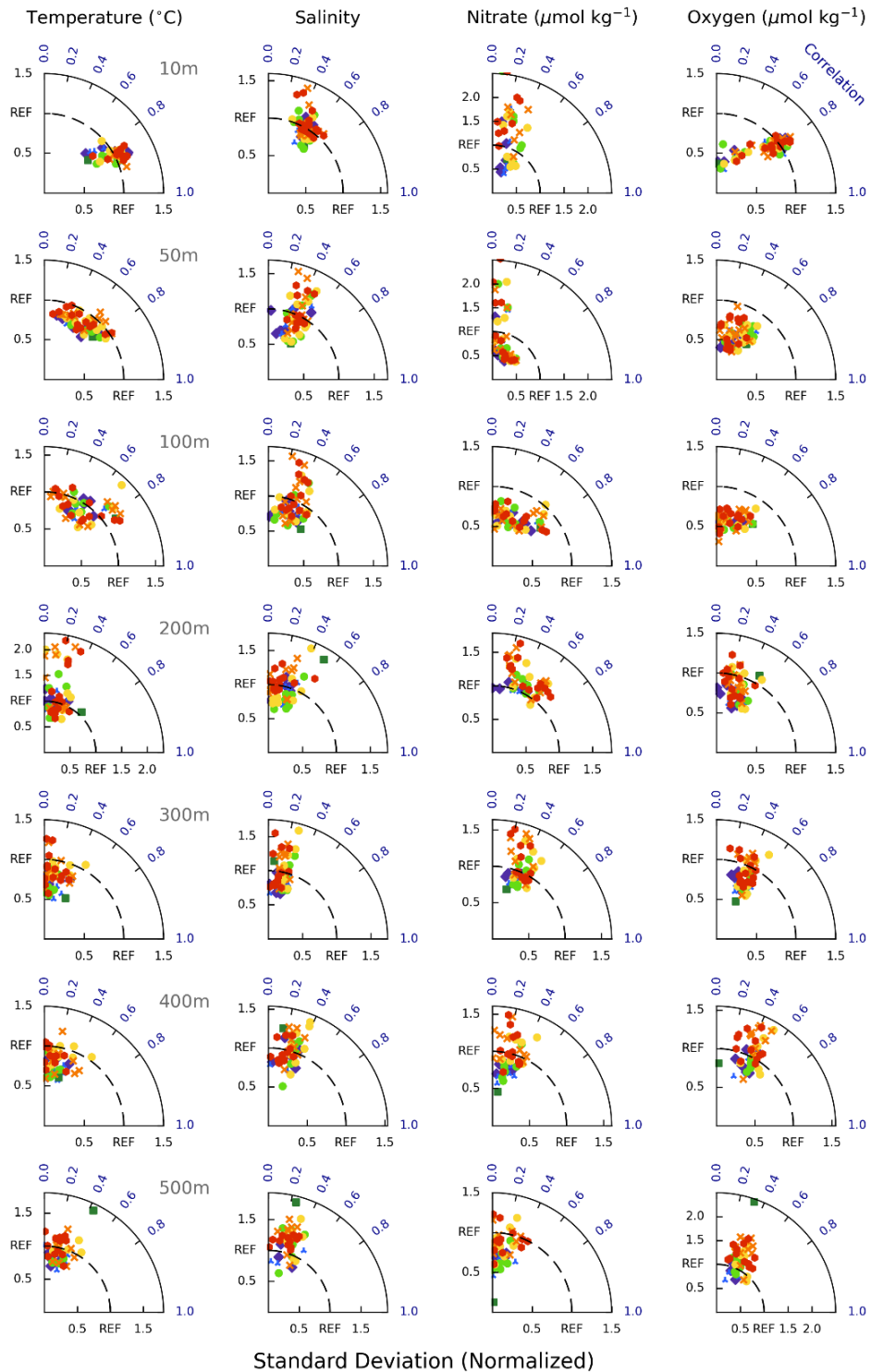


**Figure S29. Cruise-averaged NEP10k compared against CalCOFI 1993-2019 bottle data**

Taylor diagrams for NEP10k temperature, salinity, nitrate and oxygen compared against CalCOFI bottle data. For each cruise, data and regridded NEP10k output were averaged over the entire CalCOFI survey extent at each depth in order to smooth biases that might arise from mismatched placement of submesoscale features. Normalized standard deviation (standard deviation of the model values divided by that of the CalCOFI data) appears on the x and y axes; Pearson correlation coefficient is expressed as the angle above the x-axis.

